EPIC OBSERVATIONS OF BRIGHT BL LAC OBJECTS: WHAT CAN WE LEARN FROM THE X-RAY SPECTRA ABOUT THE ISM

F. Haberl[1], S. Sembay[2], B. Altieri[3], and W. Brinkmann[1]

[1]Max-Planck-Institut für extraterrestrische Physik, Giessenbachstraße, 85748 Garching, Germany
[2]Department of Physics and Astronomy, Leicester University, Leicester, UK
[3]European Space Agency, ESAC, Apartado 50727, 28080 Madrid, Spain

ABSTRACT

Bright BL Lac objects are used as calibration targets for X-ray instruments because of their relatively simple power-law type spectra. EPIC spectra with their very high statistical quality provide not only information about the shape (curvature) of the intrinsic source spectra themselves but also constrain the properties of the absorbing interstellar matter in the Galactic foreground.

In the XMM-Newton EPIC spectra of bright, low-absorbed sources like Mkn 421, PKS 2155–304 and H 1426+428 the oxygen absorption is dominated by instrumental effects. We present results from a spectral analysis of higher absorbed objects which shows that the EPIC spectra are very sensitive to oxygen, iron and neon abundances in the absorbing interstellar medium (ISM). While the oxygen abundance is consistent with that given by (Wilms et al. 2000) there are indications for a higher iron abundance. EPIC observations can be used to constrain the abundances in the ISM for fainter sources complementary to high spectral resolution spectra from bright BL Lac objects.

Key words: galaxies: active – ISM: abundances – X-rays: ISM.

1. INTRODUCTION

Within the 0.5 – 2 keV X-ray band where the sensitivity of the XMM-Newton EPIC instruments (Strüder et al. 2001; Turner et al. 2001) is highest, photo-ionization of the ISM causes absorption edges in the X-ray spectra, mainly by oxygen, iron and neon (Wilms et al. 2000). The depth of the edges can be used to constrain the abundances of the elements involved. In particular high resolution spectrographs as the XMM-Newton RGS (den Herder et al. 2001) and Chandra LETG (Brinkman et al. 2000) allow a detailed study of the oxygen K-edge (de Vries et al. 2003; Juett et al. 2004; Kirsch et al. 2005).

BL Lac objects (or blazars) are a class of active galactic nuclei (AGN) characterized by non-thermal emission which is believed to originate in a jet oriented close to the line of sight. In the X-ray band the spectra are usually represented by a single power-law, a broken power-law or a continuously curved continuum which is attenuated only by absorption in the Galactic ISM (e.g. Donato et al. 2005). Some blazars are very bright X-ray sources and together with their featureless spectrum they are ideally suited for the study of absorption edges with high spectral resolution.

Although the EPIC instruments with their medium energy resolution of $\sim$100–140 eV (full width half maximum) can not resolve absorption edges they can be used in a complementary way. Due to their unprecedented sensitivity modeling of spectra (by taking into account the structure of edges measured with high resolution) is possible for much fainter sources.

2. EPIC CALIBRATION USING BLAZARS

The EPIC as well as the high resolution instruments suffer from absorption by oxygen intrinsic to the detector. The detector intrinsic edges can be separated from the interstellar contribution by comparing spectra from sources with high and low absorption (de Vries et al. 2003). Fig. 1 shows the current status of the EPIC-pn calibration using the archival data of PKS 2155–304 and H 1426+428, two bright blazars with relatively low Galactic absorption. Some residuals at the few % level close to the instrumental edges are caused by small gain shifts. Overall, the fits are acceptable with reduced χ^2 values of 1.16 (a total of 4481 degrees of freedom, dof, from 13 spectra of PKS 2155–304) and 1.22 (2864 dof from 6 spectra of H 1426+428). The absorption in the spectra is modeled using the abundance table of Wilms et al. (2000) (see below), however, due to the low column density the fit is not very sensitive to the oxygen abundance. Column densities in the fits to blazar spectra are fixed to the Galactic value as they are derived from HI measurements and are

Table 1. A sample of elemental abundance tables.

Element	angr	feld	aneb	grsa	wilms	lodd	loddp
H	1.00	1.00	1.00	1.00	1.00	1.00	1.00
He	$9.77{\cdot}10^{-2}$	$9.77{\cdot}10^{-2}$	$8.01{\cdot}10^{-2}$	$8.51{\cdot}10^{-2}$	$9.77{\cdot}10^{-2}$	$7.92{\cdot}10^{-2}$	$9.64{\cdot}10^{-2}$
Li	$1.45{\cdot}10^{-11}$	$1.26{\cdot}10^{-11}$	$2.19{\cdot}10^{-9}$	$1.26{\cdot}10^{-11}$	0.00	$1.90{\cdot}10^{-9}$	$2.24{\cdot}10^{-9}$
B	$1.41{\cdot}10^{-11}$	$2.51{\cdot}10^{-11}$	$2.87{\cdot}10^{-11}$	$2.51{\cdot}10^{-11}$	0.00	$2.57{\cdot}10^{-11}$	$3.02{\cdot}10^{-11}$
Be	$3.98{\cdot}10^{-10}$	$3.55{\cdot}10^{-10}$	$8.82{\cdot}10^{-10}$	$3.55{\cdot}10^{-10}$	0.00	$6.03{\cdot}10^{-10}$	$7.08{\cdot}10^{-10}$
C	$3.63{\cdot}10^{-4}$	$3.98{\cdot}10^{-4}$	$4.45{\cdot}10^{-4}$	$3.31{\cdot}10^{-4}$	$2.40{\cdot}10^{-4}$	$2.45{\cdot}10^{-4}$	$2.88{\cdot}10^{-4}$
N	$1.12{\cdot}10^{-4}$	$1.00{\cdot}10^{-4}$	$9.12{\cdot}10^{-5}$	$8.32{\cdot}10^{-5}$	$7.59{\cdot}10^{-5}$	$6.76{\cdot}10^{-5}$	$7.94{\cdot}10^{-5}$
O	$8.51{\cdot}10^{-4}$	$8.51{\cdot}10^{-4}$	$7.39{\cdot}10^{-4}$	$6.76{\cdot}10^{-4}$	$4.90{\cdot}10^{-4}$	$4.90{\cdot}10^{-4}$	$5.75{\cdot}10^{-4}$
F	$3.63{\cdot}10^{-8}$	$3.63{\cdot}10^{-8}$	$3.10{\cdot}10^{-8}$	$3.63{\cdot}10^{-8}$	0.00	$2.88{\cdot}10^{-8}$	$3.39{\cdot}10^{-8}$
Ne	$1.23{\cdot}10^{-4}$	$1.29{\cdot}10^{-4}$	$1.38{\cdot}10^{-4}$	$1.20{\cdot}10^{-4}$	$8.71{\cdot}10^{-5}$	$7.41{\cdot}10^{-5}$	$8.91{\cdot}10^{-5}$
...							
Fe	$4.68{\cdot}10^{-5}$	$3.24{\cdot}10^{-5}$	$3.31{\cdot}10^{-5}$	$3.16{\cdot}10^{-5}$	$2.69{\cdot}10^{-5}$	$2.95{\cdot}10^{-5}$	$3.47{\cdot}10^{-5}$
...							

angr: Anders & Grevesse (1989) (default in XSPEC v11.3)
feld: Feldman (1992)
aneb: Anders & Ebihara (1982)
grsa: Grevesse & Sauval (1998)
wilms: Wilms et al. (2000)
lodd: Lodders (2003), solar photospheric
loddp: Lodders (2003), proto-solar (not in XSPEC v11.3)

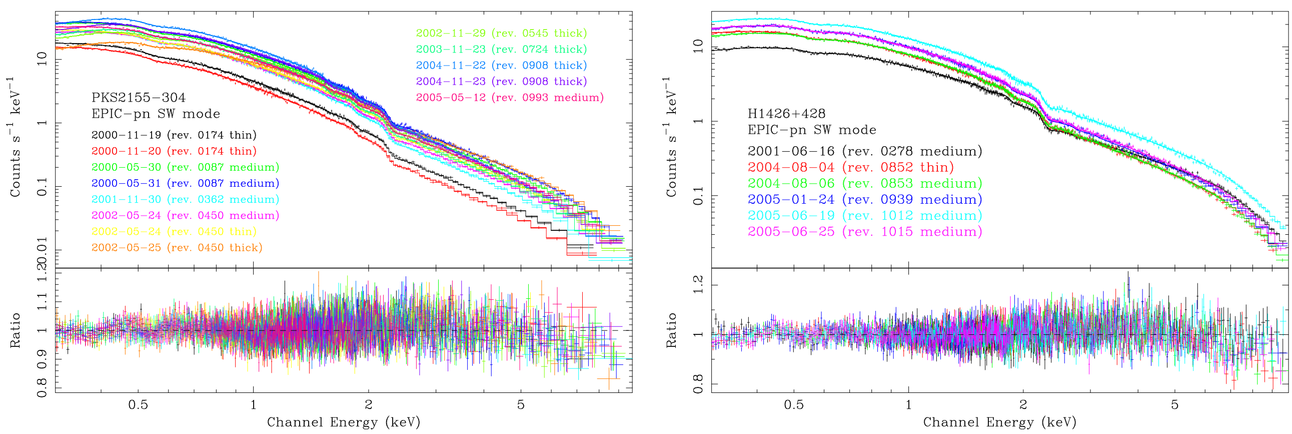

Figure 1. Broken power-law fits to the EPIC-pn spectra of PKS 2155–304 and H 1426+428. The absorption column density is fixed at the Galactic value derived from HI measurements (1.43·10^{20} cm^{-2} for PKS 2155–304 and 1.36·10^{20} cm^{-2} for H 1426+428). Intensity and power-law slopes vary with time for both sources.

taken from Lockman & Savage (1995), Elvis et al. (1989) or Dickey & Lockman (1990).

3. ELEMENTAL ABUNDANCES IN THE ISM

Since the commonly used elemental abundance table by Anders & Grevesse (1989) was compiled, many updates were published (examples can be found in Table 1). It was noted that photospheric abundances are not equal to the abundances representative for the whole solar system due to possible heavy-element settling in the sun (Lodders 2003). These proto-solar abundances might be more appropriate to use for modeling the X-ray absorption along the line of sight at least towards nearby X-ray sources. However, abundance gradients may exist in the Galaxy and the study of X-ray absorption in the spectra of blazars at various positions on the sky is important to constrain line of sight averaged abundances of the most abundant elements like oxygen and iron.

3.1. Higher absorbed blazars

We have started to investigate a sample of higher absorbed ($N_H \sim 10^{21}$ cm^{-2}) blazars in order to constrain the oxygen abundance along their lines of sight. Deeper absorption edges are more easily to measure with medium resolution instruments. The first two blazars appropriate for our study and available in the XMM-Newton archive are H 0414+009 (observed during satellite revolution 683) and 1ES 1959+65.0 (revolutions 568 and 580). The model fit using an absorbed broken power-law with the “angr” (see Table 1) abundance table results for both sources in residuals around the O-edge. The residuals are similar in shape to a “negative” absorption edge (see Figs. 2 and 3), which suggests that the assumed oxygen abundance is overestimated. This is confirmed by allowing the oxygen abundance to vary in the fit which results in a lower oxygen column density. Using other abundance tables which involve a lower oxygen abundance in the first place yield improved fits, but there is indication for an even somewhat more reduced O abundance for both sources. Table 2 summarizes the results for the oxygen abundances derived from fits to the EPIC-pn spectra for a sample of available abundance tables. For the line of sight to H 0414+009 the oxygen abundance appears to be lower than the minimum value from the different values found in Table 1. Moreover, there is indication for different O abundances towards the two sources with a somewhat lower value found from 1ES 1959+65.0.

3.2. Galactic sources

In principle also Galactic sources with simple continuum spectra can be used for our study. The equivalent hydrogen column density is an additional free parameter in the spectral fits. As example we show the EPIC spectra of the anomalous X-ray pulsar 1E2259+586 in Fig. 4. The equivalent hydrogen column density of $\sim 10^{22}$ cm^{-2} is so high that most of the emission below the O-edge is absorbed away. Similar to the blazars investigated above, a reduced O-abundance improves the fit significantly (Table 2). Further, there is evidence for an Fe abundance lower than that included in the “angr” table (0.839$\pm$0.095), but higher than in the “wilms” table (1.396$\pm$0.177). There may be also potential to constrain neon abundances, however, the calibration of the EPIC instruments needs to be improved around 1 keV as the discrepancy between pn and MOS shows.

4. A NARROW ABSORPTION LINE

The EPIC-pn spectra of PKS 2155–304 and H 1426+428 show evidence for a narrow absorption line at 1.8 keV, just below the Si-K edge. Investigations of spectra of other AGN confirm the presence of the feature and revealed differences in the depth of the line for various sources. The strongest line was found at 1823$\pm$7 eV in the spectrum of MCG-6-30-15 (Fig. 5, left) which is also attenuated by the largest Galactic absorption in our sample of investigated sources, while there is only marginal evidence for such a line in the spectrum of Mkn 421 (Fig. 5, right). The different line equivalent widths argue against a detector-intrinsic Si feature and the line is also indicated in EPIC-MOS of MCG-6-30-15 although with lower significance due to the larger Si absorption edge.

5. CONCLUSIONS

The analysis of EPIC spectra of blazars has demonstrated the possibility to measure oxygen abundances along various lines of sight throughout the Galaxy. First results derived from X-ray spectra of H 0414+009 and 1ES 1959+65.0 show that oxygen is less abundant than given by older abundance tables (e.g. Anders & Grevesse 1989; Feldman 1992). Newer tables by Wilms et al. (2000) and Lodders (2003) include reduced ($\sim$60%) oxygen abundances more consistent with our measurements, although we find evidence for even lower oxygen abundances at least in the directions of the two blazars. In addition we find evidence for different oxygen abundances in the two directions. Clearly more X-ray spectra of sources at different positions in the sky need to be investigated to constrain abundance gradients in the ISM.

A narrow absorption line near 1.82 keV is observed in the spectra of several AGN, the strongest case we found being MCG-6-30-15. We identify this line with the 1.821 keV line transition of Fe XXIV which exhibits its highest emissivity in the temperature range of 1.5 to 2.5 keV. Another Fe XXIV line transition at 1.164 keV was identified in RGS spectra of MCG-6-30-15 together with lines from other Fe ions (XVII-XXII) by Turner et al. (2004). All the measured line energies are consistent with their rest energies strongly suggesting an origin in the Milky

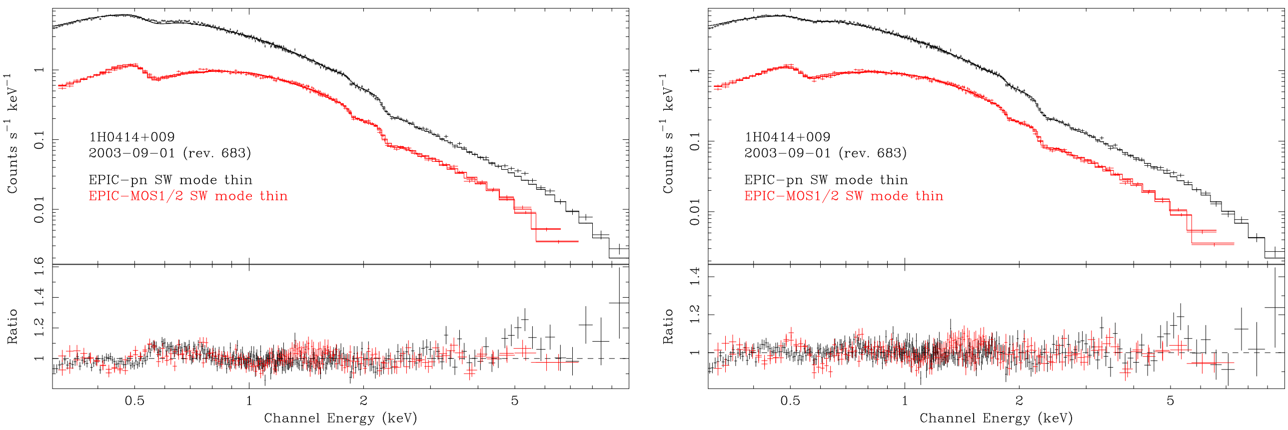

Figure 2. Broken power-law fits to the EPIC-pn and EPIC-MOS spectra of H 0414+009. The absorption column density is fixed at the Galactic value of 9.15·10^{20} cm^{-2}. Left: Abundances "angr", right: "loddp" with free oxygen abundance.

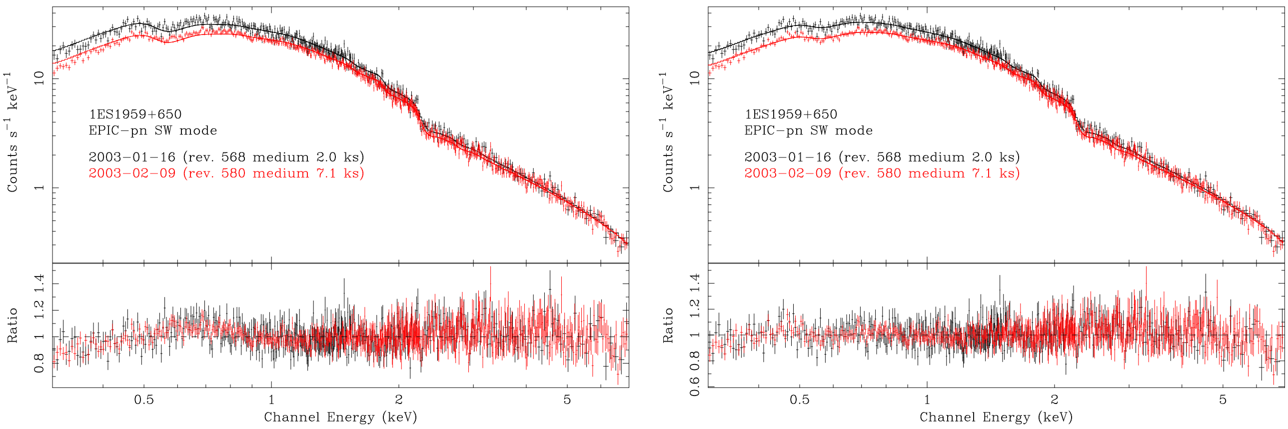

Figure 3. Broken power-law fits to EPIC-pn spectra of 1ES 1959+650. The absorption column density is fixed at the Galactic value of 9.89·10^{20} cm^{-2}. Left: Abundances "angr", right: "wilms" with free oxygen abundance.

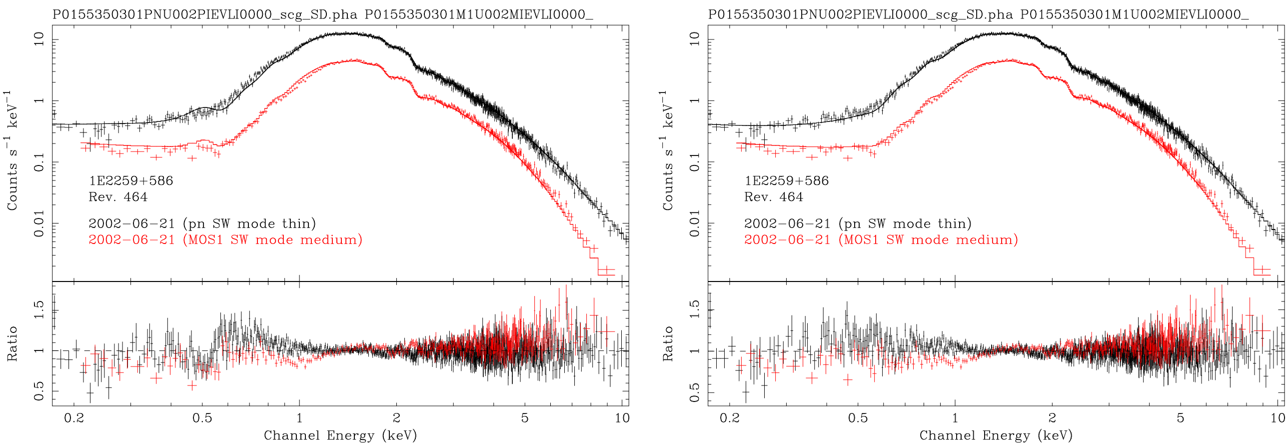

Figure 4. Two component (bremsstrahlung+power-law) fits to the EPIC spectra of 1E2259+566 using different abundance tables. Left: "angr", right: "wilms" with O and Fe abundance as free parameters.

Table 2. A sample of elemental abundance tables.

	oxygen abundance relative	relative/H	χ^2	dof	χ^2_r
H 0414+009					
angr	1.0 fix	$8.51\cdot10^{-4}$ fix	493	308	1.600
wilms	1.0 fix	$4.90\cdot10^{-4}$ fix	319	307	1.040
lodd	1.0 fix	$4.90\cdot10^{-4}$ fix	352	307	1.148
loddp	1.0 fix	$5.75\cdot10^{-4}$ fix	327	307	1.065
angr	0.599±0.054	$5.10\cdot10^{-4}$	315	306	1.029
wilms	0.865±0.090	$4.24\cdot10^{-4}$	313	306	1.024
lodd	0.714±0.099	$3.50\cdot10^{-4}$	334	306	1.091
loddp	0.801±0.079	$4.61\cdot10^{-4}$	312	306	1.019
1ES 1959+65.0					
angr	1.0 fix	$8.51\cdot10^{-4}$ fix	1351	1010	1.600
wilms	1.0 fix	$4.90\cdot10^{-4}$ fix	1187	1009	1.040
lodd	1.0 fix	$4.90\cdot10^{-4}$ fix	1267	1010	1.148
loddp	1.0 fix	$5.75\cdot10^{-4}$ fix	1194	1010	1.065
angr	0.528±0.066	$4.49\cdot10^{-4}$	1144	1008	1.029
wilms	0.709±0.118	$3.47\cdot10^{-4}$	1170	1008	1.024
lodd	0.541±0.118	$2.65\cdot10^{-4}$	1219	1008	1.091
loddp	0.671±0.100	$3.86\cdot10^{-4}$	1161	1008	1.019
1E2259+566					
angr	1.0 fix	$8.51\cdot10^{-4}$ fix	1194	980	1.218
wilms	1.0 fix	$4.90\cdot10^{-4}$ fix	1129	980	1.153
angr	0.574±0.087	$4.88\cdot10^{-4}$	1077	978	1.101
wilms	0.625±0.209	$3.06\cdot10^{-4}$	1076	978	1.111

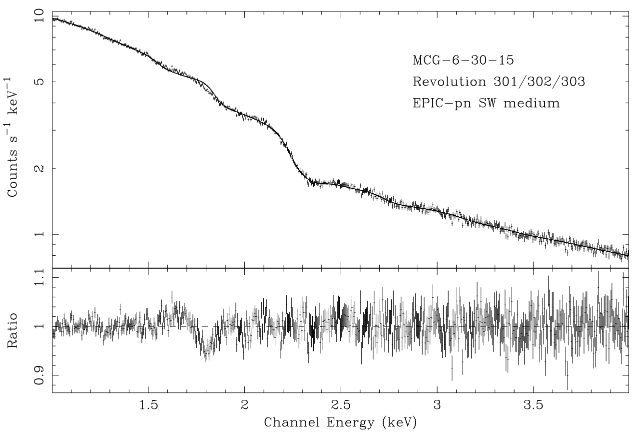

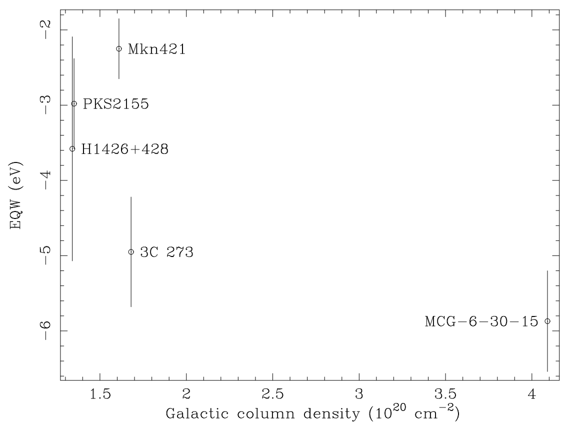

Figure 5. Left: Power-law fit to the merged EPIC-pn spectrum in the 1-4 keV band obtained in satellite revolutions 301, 302 and 303. A highly significant feature at 1.8 keV is visible in the residuals which can be modeled by a narrow absorption line. Right: Equivalent width of the 1.8 keV absorption line for a sample of extra-galactic sources. There is some evidence that the line is deeper for sources with higher Galactic column density.

Way in hot (up to ∼2.5 keV) gas. Such temperatures in the interstellar gas can easily be reached by supernova explosions and the interaction of supernova remnants with the ISM.

ACKNOWLEDGMENTS

The XMM-Newton project is supported by the Bundesministerium für Bildung und Forschung / Deutsches Zentrum für Luft- und Raumfahrt (BMBF / DLR), the Max-Planck-Gesellschaft and the Heidenhain-Stiftung. This work is based on the efforts of the whole XMM-Newton EPIC calibration team.

REFERENCES

Anders, E. & Ebihara, M. 1982, Geochim. Cosmochim. Acta, 46, 2363

Anders, E. & Grevesse, N. 1989, Geochim. Cosmochim. Acta, 53, 197

Brinkman, A. C., Gunsing, C. J. T., Kaastra, J. S., et al. 2000, ApJ, 530, L111

de Vries, C. P., den Herder, J. W., Kaastra, J. S., et al. 2003, A&A, 404, 959

den Herder, J. W., Brinkman, A. C., Kahn, S. M., et al. 2001, A&A, 365, L7

Dickey, J. M. & Lockman, F. J. 1990, Ann. Rev. Astron. Astrophys., 28, 215

Donato, D., Sambruna, R. M., & Gliozzi, M. 2005, A&A, 433, 1163

Elvis, M., Lockman, F. J., & Wilkes, B. J. 1989, AJ, 97, 777

Feldman, U. 1992, Physica Scripta Volume T, 46, 202

Grevesse, N. & Sauval, A. J. 1998, Space Science Reviews, 85, 161

Juett, A. M., Schulz, N. S., & Chakrabarty, D. 2004, ApJ, 612, 308

Kirsch, M. G. F., Briel, U. G., Burrows, D., & et al. 2005, in Proceedings of the SPIE, 2005

Lockman, F. J. & Savage, B. D. 1995, ApJS, 97, 1

Lodders, K. 2003, ApJ, 591, 1220

Strüder, L., Briel, U., Dennerl, K., et al. 2001, A&A, 365, L18

Turner, A. K., Fabian, A. C., Lee, J. C., & Vaughan, S. 2004, MNRAS, 353, 319

Turner, M. J. L., Abbey, A., Arnaud, M., et al. 2001, A&A, 365, L27

Wilms, J., Allen, A., & McCray, R. 2000, ApJ, 542, 914